J. Cent. South Univ. (2023) 30: 1345−1358
DOI: https://doi.org/10.1007/s11771-023-5289-5

Springer

Tensile failure and acoustic emission characteristics of rock salt under different tensile testing conditions

LIU Jian-feng(刘建锋)[1], WANG Chun-ping(王春萍)[1, 2], WANG Lu(王璐)[1, 3]*,
RAN Li-na(冉莉娜)[1, 4], DENG Chao-fu(邓朝福)[1]

1. State Key Laboratory of Hydraulics and Mountain River Engineering, Sichuan University, Chengdu 610044, China;
2. Beijing Research Institute of Uranium Geology, Beijing 100822, China;
3. School of Architecture and Civil Engineering, Xihua University, Chengdu 610039, China;
4. CNPC Key Laboratory of Oil and Gas Underground Storage Engineering, Langfang 065007, China

Abstract: The tensile strength of rock salt is an important parameter in the salt cavern gas storage project. Due to the high requirements for experimental setup and rock specimens in the direct tensile test, it is necessary to find another alternative to obtain the tensile strength. Therefore, the tensile strength and acoustic emission (AE) characteristics obtained by the direct tensile test, Brazilian test with simplified ISRM standard, Brazilian test with China standard, and three-point-bending test were discussed in this paper. It is noticed that the tensile testing method has an effect on the tensile strength of rock salt and the AE counts, energy and spatial distribution. Based on the tensile strength determined by three-point-bending test and the AE evolution characteristics, the indirect tensile strength determined by three-point-bending test was much closer to the tensile strength determined by direct tensile test, meaning that the three-point-bending test could be considered as a good option to obtain the tensile strength of rock salt except direct tensile test.

Key words: rock salt; tensile strength; acoustic emission; damage evolution

Cite this article as: LIU Jian-feng, WANG Chun-ping, WANG Lu, RAN Li-na, DENG Chao-fu. Tensile failure and acoustic emission characteristics of rock salt under different tensile testing conditions [J]. Journal of Central South University, 2023, 30(4): 1345−1358. DOI: https://doi.org/10.1007/s11771-023-5289-5.

1 Introduction

Rock salt is characterized by low porosity, high ductility, low permeability, self-healing ability and good creep properties. Since the late 1940s, salt caverns have been used for the underground storage of oil, natural gas, petroleum and compressed air and disposal of radioactive and chemical wastes [1−3]. Accordingly, extensive experimental and theoretical investigations on the fundamental mechanical properties under different stress conditions, the deformation mechanisms and microstructural development of rock salt have been conducted [4−6]. Since the tensile strength of rock material dictates and controls the maximum internal pressure of unlined underground caverns and the maximum roof span of underground structures, a good understanding of the tensile behavior of rock salt is essential to the design and long-term stability and safety analysis of the underground project.

For the past few decades, experimental studies

Foundation item: Projects(2022YFSY0007, 2021YFH0010) supported by the Scientific and Technological Research Projects in Sichuan Province, China
Received date: 2022-07-19; **Accepted date:** 2022-11-01
Corresponding author: WANG Lu, PhD, Lecturer; E-mail: homewanglu@163.com; ORCID: https://orcid.org/0000-0002-3836-6185

have been conducted to investigate the tensile mechanical properties of rock salt [7 − 9]. In the safety evaluation of salt cavern gas storage, researchers determined the tensile strength of Jintan rock salt by Brazilian disk splitting tests [10]. Based on a series of direct tensile tests and Brazilian tests, the tensile strength of bedded rock salt and the relationship between direct and indirect tensile methods were determined and proposed [11]. In addition, the three-point bending test is also an alternative to study the tensile strength and fracture toughness of rocks. In the three-point bending test, the bending tensile stress presents a triangular load distribution on the section. The tensile stress at the tip reaches the maximum and decreases toward the middle of the specimen. Theoretically, the tensile strength derived from the material mechanics bending strength theory has high reliability. Therefore, based on the maximum load measurements from notched three-point-bending tests, both tensile strength and fracture toughness of rock or concrete can be determined [12−13].

In general, the laboratory testing methods for investigating the tensile behavior of rocks are not unique, which can be generally classified as direct tension method and indirect tension method. The direct tensile test is the most fundamental and straightforward method for determining the tensile strength of rocks. However, the laboratory test has high requirements for the experimental set-up and samples [14]. For instance, the specimen's two end surfaces should be strictly parallel and perpendicular to the axial line of the specimen. The axial lines of the testing machine, the measurement device and the sample should be completely aligned. Otherwise, it is hard to successfully derive accurate testing results [15]. Profited from the convenience and flexibility of testing machine, the indirect tension methods, particularly the Brazilian test and flexural test such as three- and four-point-bending tests are widely adopted [16−20]. However, there are many assumptions to successfully implement the indirect tension methods, such as two-dimensional plane simplification, homogeneous material, and linear elastic behavior before brittle failure [20]. Thus, some researchers are suspicious of the feasibility and accuracy of those indirect tension method in determining rock tensile strength [21 − 22]. Moreover, the set-up and loading process of the same indirect tension method may be different according to the standards in different countries. For example, according to the International Society for Rock Mechanics (ISRM) standard, two steel loading jaws with a radius of 1.5 times the specimen's radius should be applied in contact with the disk specimen in Brazilian test [23]. In China standard, two steel bars with 1 mm diameter should be employed in Brazilian test [24−25]. Consequently, different testing results may be derived. Since the stress distribution or effective volumes are different in different tension methods, significant differences can be observed in the tensile strengths determined from different tensile tests, and even in the relationship between the direct tensile strength and indirect tensile strength for different rock materials [26−27]. Moreover, the investigation conducted on rock salt to identify the effect of tensile testing method on the peak stress at rock failure is very limited.

The objective of this work is to investigate the tensile strength of rock salt. Three types of tensile test, i.e., direct tensile test, Brazilian test and three-point-bending test were carried out. When carrying out the Brazilian test, two methods were adopted, namely Brazilian test with simplified ISRM standard and Brazilian test with China standard. The relationship between tensile strength values determined from different tension methods was discussed. In order to study the damage evolution characteristics during the three types of tensile test, the loading − unloading cycles were also performed in each type of the tests. The microcracking processes induced by different tension methods were detected by a 3D acoustic emission test system.

2 Experimental

The rock specimen adopted in this study is pure rock salt, with a salt content more than 90.00%. The rock specimens for tensile tests were prepared following the standard of Ref. [24]. Three types of tensile tests were conducted including direct tensile test, Brazilian test and three-point-bending test. The cylindrical specimen in direct tensile test is adopted with a diameter of 100.0 mm and a height of 100.0 mm. For the Brazilian test, the flattened disc specimen is 90.0 mm in diameter and 45.0 mm in thickness. For three-point-bending test,

the specimen is cuboid with 210.0 mm in length, 100.0 mm in height and 50.0 mm in width. A notch is carefully introduced at the center of the bottom surface of specimen with 15.0 mm in depth and 1.5 mm in width.

The tensile tests were carried out on a MTS815 rock mechanics test system. The axial loading capacity for compression is 4600 kN. Figure 1 shows the experimental setup for different tensile tests. In direct tensile test, the device with position-limit spring for alternating tension − compression cyclic test [28] is used (Figure 1(a)). The experimental device is developed by our research team which can provide a completely reversed loading condition: direct tensile stress and compressive stress, which can be easily applied for investigating the tensile behavior of rock material (LIU et al 2019 [14]). The axial displacement is measured by two linear variable differential transformers (LVDT). In the direct tensile test, the axial LVDT is used to control the tensile rate to be 0.01 mm/min. Considering the influence of the loading and unloading stress paths in the salt cavern reservoir on rock salt, and in order to reveal the damage evolution characteristics of rock salt under different tensile methods, loading and unloading are performed before the peak until the tensile stress reached about 80% of the peak stress. And then, in order to obtain the post-peak deformation curve, the control rate is reduced to 0.001 mm/min until a complete stress−strain curve is obtained.

For Brazilian test, the experimental set-up suggested by China standard is different from that suggested by ISRM standard. In order to compare the feasibility of these two standards in determining the tensile strength of rock salt, two testing methods, namely Brazilian test with simplified ISRM standard and Brazilian test with China standard, are adopted. As presented in Figure 1(b), the Brazilian test with simplified ISRM standard is performed by replacing the two steel jaws in the ISRM standard by two flat steel cushions. In Brazilian test with China standard (Figure 1(c)), two steel bars are placed between the flat steel plate and the rock specimen to provide a symmetric line loading. The Brazilian test is controlled by LVDT with the rate of 0.3 mm/min for both loading and unloading, and the lower limit load of unloading is 0.3 kN. Loading and unloading cycles were performed about every 0.5 kN before the peak, and 4−5 loading and unloading cycles were carried out after the peak.

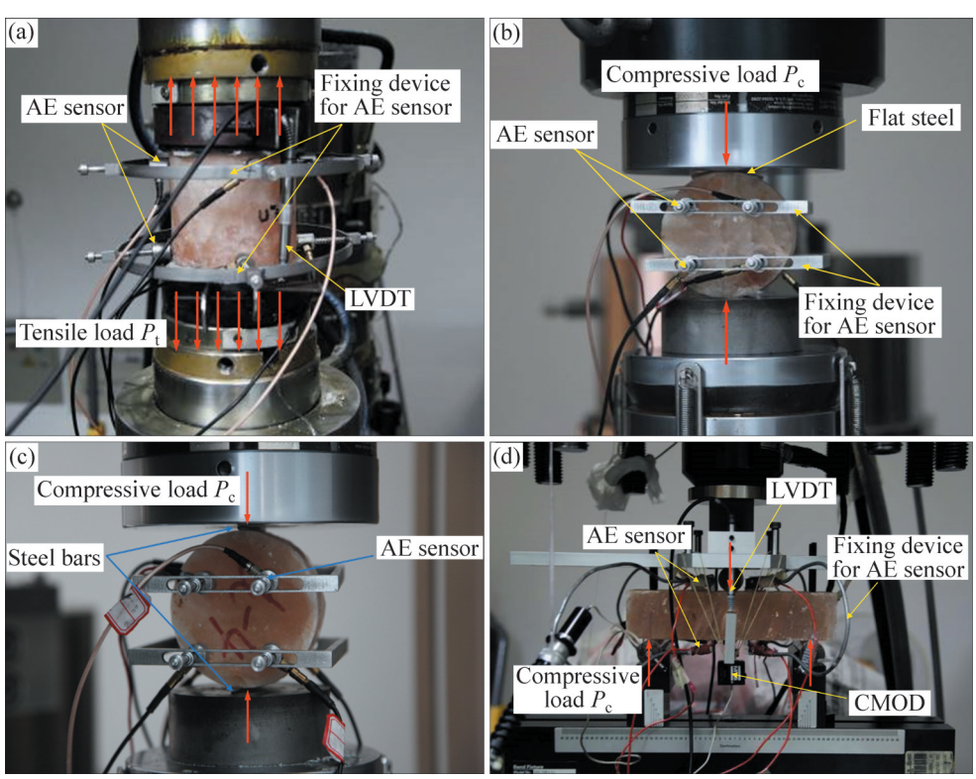

Figure 1 Illustration of experimental setup for different tensile tests: (a) Direct tensile test; (b) Brazilian test with simplified ISRM standard; (c) Brazilian test with China standard; (d) Three-point-bending test

The compression in three-point-bending test is applied along the top centerline of the rock specimen, with two supports close to the ends at bottom (Figure 1(d)). The span between supports is 160 mm. The load point displacement is measured by LVDT. During the test, loading and unloading are controlled by the crack mouth opening displacement (CMOD) with 0.1 mm/min of the notch opening displacement rate. The lower limit load of unloading was 0.1 kN.

During the three types of tensile test, a 3D acoustic emission system is employed to record the initiation and propagation process of microcracks inside the specimen. Eight Micro30 AE sensors are fixed on the surface of the rock salt specimen through the fixing device developed by our research team (Figure 1) [14]. According to the lead break test before the tensile tests, the parameters of the AE sensors are selected with a working frequency of 150 kHz, a threshold of 30 dB and a preamplifier gain of 40 dB.

In direct tensile test, the direct tensile strength σ_{dt} can be calculated from the equation:

$$\sigma_{dt}=\frac{P_t}{A} \tag{1}$$

where P_t is the peak tensile load; A is the cross sectional area of the specimen.

In Brazilian test, the disc specimen is compressed between two flat plates (or flat plates with steel bars), which provides compressive load along the diameter direction of the specimen. The indirect tensile strength σ_{bt} can be calculated as [24]:

$$\sigma_{bt}=\frac{2P_c}{\pi DH} \tag{2}$$

where P_c is the peak compressive load; D and H are the diameter and thickness of the disc specimen, respectively.

In three-point-bending test, the compression is applied along the centerline of the rock specimen, and the indirect tensile strength can be estimated by the maximum compressive load. The fracture will firstly occur at the tip of the notch. For simplicity, the compressive stress at the loading point is equal to the tensile stress at the tip of the notch at the peak compressive load P_c. The indirect tensile strength for three-point-bending test σ_{tt} can be estimated by [12−13]:

$$\sigma_{tt}=\frac{3P_cS}{2K(L-a)^2} \tag{3}$$

where S is the span between supports; K is the width of specimen; L and a refer the height of the specimen and the depth of the notch.

The tensile strength of rock salt determined from direct and indirect tensile tests is listed in Table 1. In order to comprehensively reflect the influence of loading and unloading stress paths on the tensile strength of rock salt during the design, construction and operation of the salt cavern gas storage project, and to effectively compare and analyze the tensile strength measured by different tensile test, the average value of the maximum tensile stress obtained under monotonic loading and loading − unloading cycles is taken as a comprehensive index in this paper, which is listed in Table 1 as “average strength”. The average tensile strength of rock salt determined by direct tensile test is 0.84 MPa. The indirect tensile strength determined by three-point-bending test is 0.81 MPa, which is much closer to the tensile strength determined by direct tensile test. The indirect tensile strength determined by Brazilian test is the highest, which is 1.97 MPa in Brazilian test with simplified ISRM standard and 1.15 MPa in Brazilian test with China standard. Figure 2 shows the representative stress − strain curves or load − displacement curves obtained from different tensile tests. It can be noticed that the axial strain at peak stress induced by direct tensile test is the smallest among the three types of tensile test. The highest axial deformation is induced by Brazilian test. The inconsistent results of tensile strength and deformation are allowed, since the stress distribution or effective volumes are different in different tensile methods.

Different from direct tensile test, in which the rock specimen is completely under a tensile stress condition, the compressive deformation may also be induced in Brazilian test and three-point-bending test. Particular to Brazilian test, the deformation in vertical direction is induced not only by the tensile fracture occurred at the center of the disc specimen but also by the compression − tensile fracture occuring at the contact surface between the plate and specimen. For rock salt, it has abundant capacity of compression − tensile deformation. The contact area between plate and specimen is

Table 1 Experimental results from direct and indirect tensile tests

Experimental type		Specimen No.	Peak load/kN	Tensile strength/MPa	Average strength/MPa
Direct tensile test		UT-1	6.48	0.83	0.84
		UT-2	6.61	0.84	
		UT-3	6.05	0.77	
		UT-4	6.18	0.79	
		UT-5	7.42	0.95	
Brazilian test	With simplified ISRM standard	d-1	12.53	1.93	1.97
		d-2	13.96	2.19	
		d-3	11.43	1.79	
	With China standard	f-1	6.03	0.95	1.15
		f-2	6.58	1.03	
		f-3	9.11	1.38	
		f-4	7.53	1.18	
		f-5	7.54	1.19	
Three-point-bending test		b-1	1.21	0.86	0.81
		b-2	0.91	0.68	
		b-3	1.20	0.89	
		b-4	0.97	0.74	
		b-5	1.08	0.87	

observed to increase significantly with the increase of loading stress. Consequently, the axial strain in Brazilian test is relatively high. Moreover, the large contact surface allows an end restraint effect to the rock specimen in Brazilian test, which leads to a relatively high tensile strength. For Brazilian test with China standard, the two steel bars placed between the plate and specimen may cause the stress concentration near the loading surface. Therefore, the tensile strength determined by Brazilian test with China standard is lower than that determined by Brazilian test with simplified ISRM standard.

Based on the loading − unloading cycles performed at different stress levels, the damage of rock salt during the three types of tensile tests is calculated. The damage is estimated by [29]:

$$D = 1 - \left(1 - \frac{\varepsilon_p}{\varepsilon}\right)\frac{\tilde{E}}{E} \tag{4}$$

where E is the initial undamaged elastic modulus, which is equal numerically to the slope of the tangent to the stress − strain curve at the onset of loading; $\tilde{E}$ is the elastic modulus with damage, which is equal numerically to the unloading modulus in each unloading stage; ε is the maximum axial strain in each loading−unloading cycle, and ε_p is the inelastic strain after each unloading.

In Eq. (4), the degradation of elastic modulus and accumulation of inelastic strain are both considered in the calculation of damage. Figure 3 shows the damage evolution process of rock salt during different tensile tests (taking specimens UT-3, d-3, f-2 and b-2 as examples). It can be noticed that the damage in different tensile tests all experiences a process of rapid increasing first at low stress levels, and then slow increasing when the damage is accumulated to some extent. The damage degree where the damage rate starts to decrease is higher than 0.8 in direct tensile test, Brazilian test with China standard and three-point-bending test, but lower than 0.6 in Brazilian test with simplified ISRM standard. The Brazilian test with simplified ISRM standard determines the highest tensile strength, and also the smallest damage. This result may be attributed to end restraint effect induced by the contact surface between the plate and the specimen, which may restrict the development of the tensile fracture and lead to a relatively high tensile strength. The highest damage is determined by three-point-bending test, corresponding to the smallest tensile strength. In direct tensile test, the inelastic strain is very small and the degradation of elastic modulus dominates the evolution of damage.

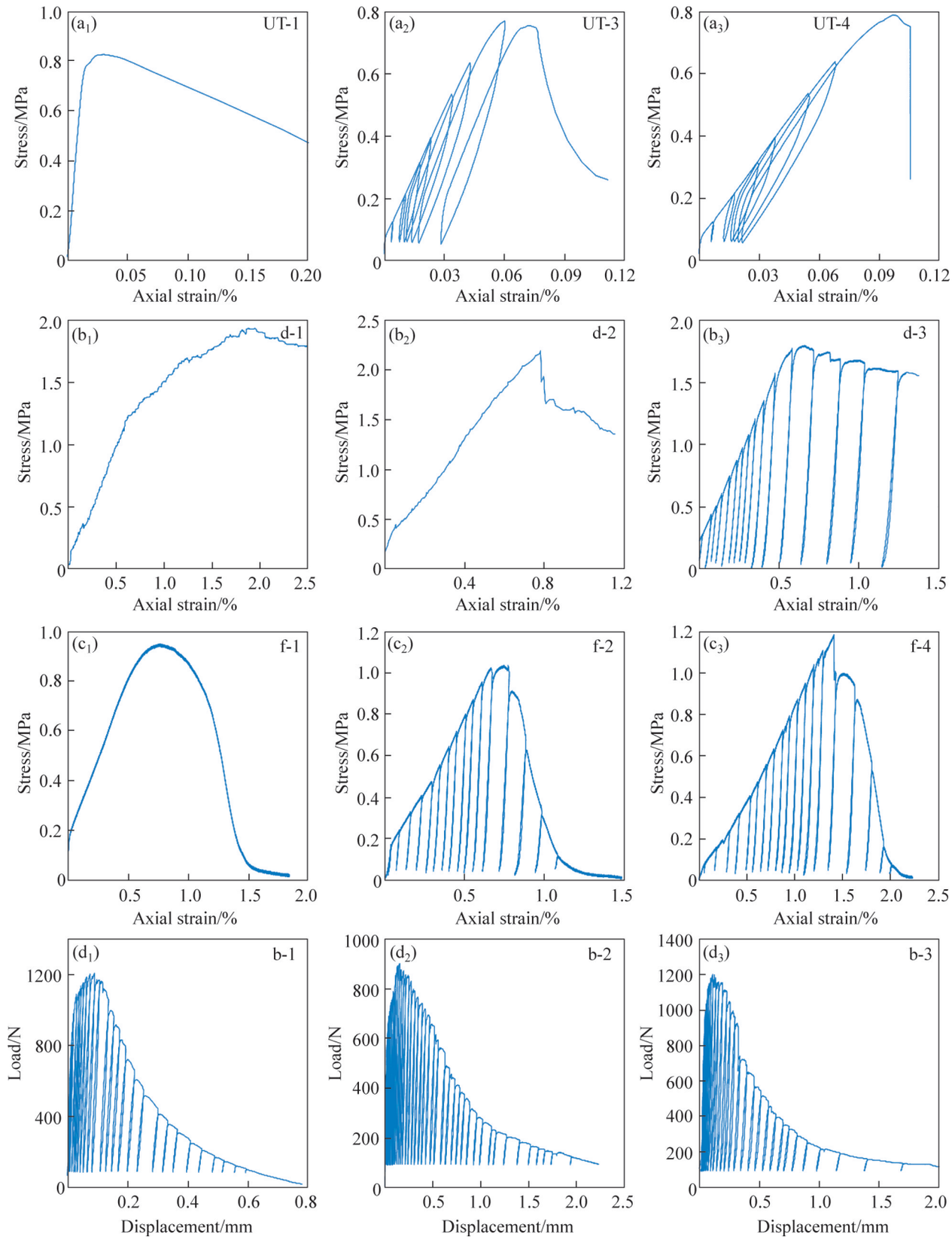

Figure 2 Stress−strain curves and load−displacement curves of different tensile tests: (a) Direct tensile test; (b) Brazilian test with simplified ISRM standard; (c) Brazilian test with China standard; (d) Three-point-bending test

However, in Brazilian test and three-point-bending test, the inelastic deformation after one loading − unloading cycle is more evident, which may play the main part in the evolution of damage.

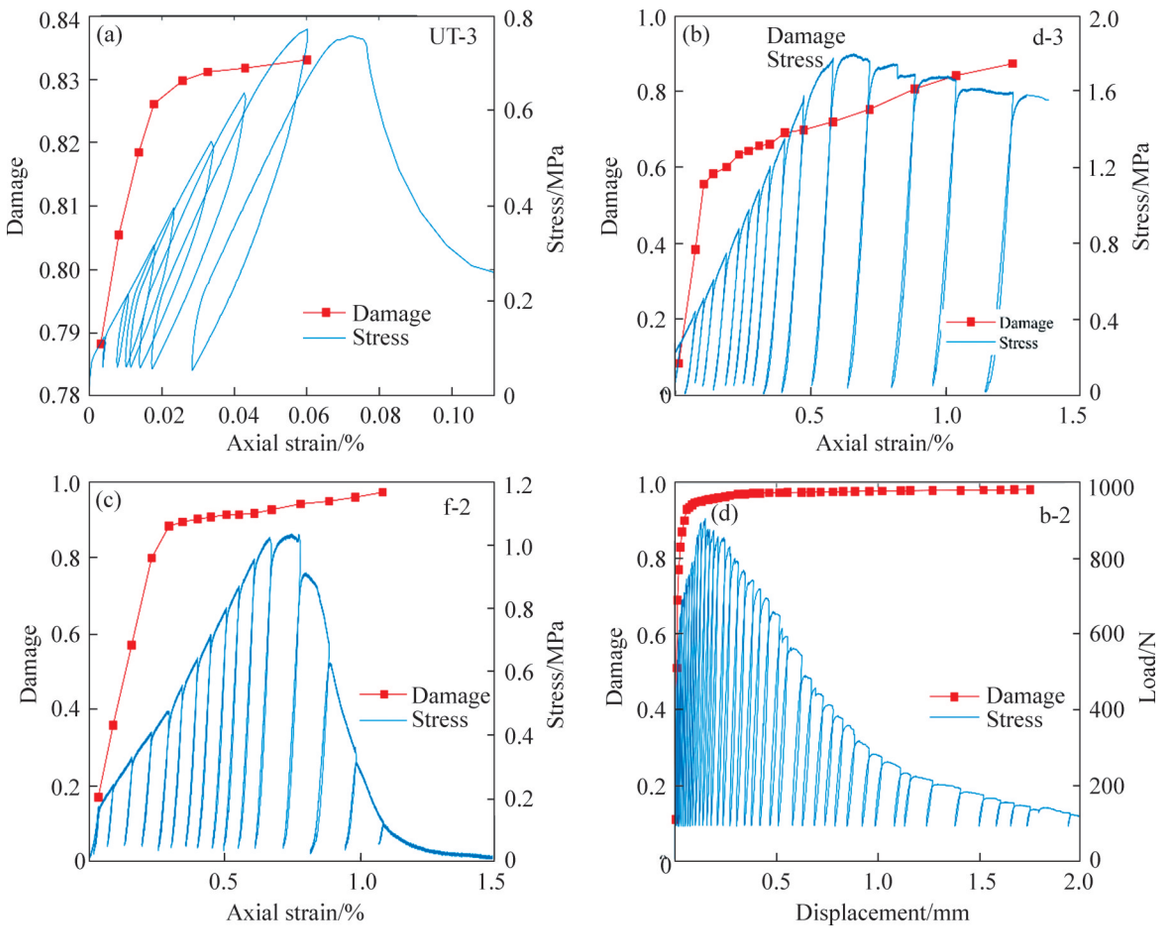

Figure 3 Damage evolution process during different tensile tests: (a) Direct tensile test; (b) Brazilian test with simplified ISRM standard; (c) Brazilian test with China standard; (d) Three-point-bending test

3 Acoustic emission characteristics

Since the acoustic emission characteristics of rock salt in the same tensile test showed good consistency, Figures 4 and 5 give the representative curves of different tensile tests. Figure 4 presents the evolution of cumulative AE counts and AE energy rate in different tensile tests. The spatial distribution of AE events at different loading stages (different percentages of the peak stress P) is shown in Figure 5. In direct tensile test, the monitored AE signal is weak and the number of AE events is very limited in the early loading stage (0–50%P). With increasing tensile stress (50%–70%P), some AE events with low energy are recorded (Figure 4(a)) and widely distributed inside the specimen (Figure 5(a)). When the loading is close to the peak stress (70%–100%P), a large amount of AE events with high energy are detected and there is a rapid increase in the cumulative AE counts. The AE events mainly concentrate along the failure surface as presented in Figure 5(a).

As presented in Figures 4(b) and (c) and Figures 5(b) and (c), AE events are observed in the early loading stage (0–25%P) of the Brazilian test. The AE events are mainly localized at the compressive zone near the loading surface at the beginning of the test, which could be attributed to the close of the intrinsic microcracks inside the specimen under compression. Then the occurrence of AE events is accelerated and the cumulative AE counts grow continuously with increasing loading stress (Figures 4(b) and (c)). It is noticed that the cumulative AE counts in both two kinds of Brazilian tests are much higher than those in the direct tensile test and three-point-bending test. The number of the cumulative AE counts is the highest in the Brazilian test with simplified ISRM standard due to the large area of compression–shear failure at the end of the specimen, resulting in a large number of AE counts.

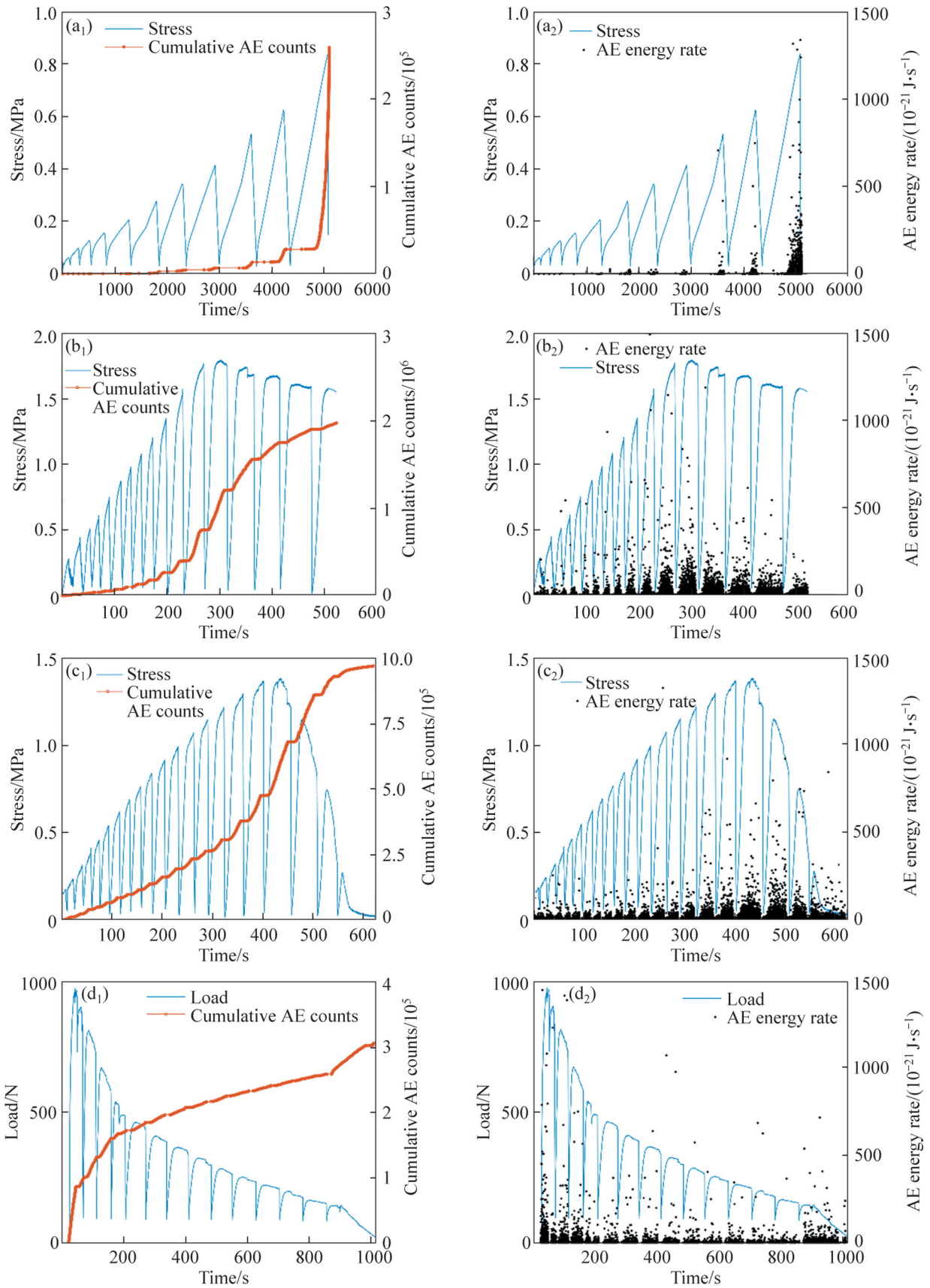

Figure 4 Variation of cumulative AE counts (a_1–d_1) and energy rate (a_2–d_2) in different tensile tests: (a) Direct tensile test (UT-2); (b) Brazilian test with simplified ISRM standard (d-3); (c) Brazilian test with China standard (f-3); (d) Three-point-bending test (b-4)

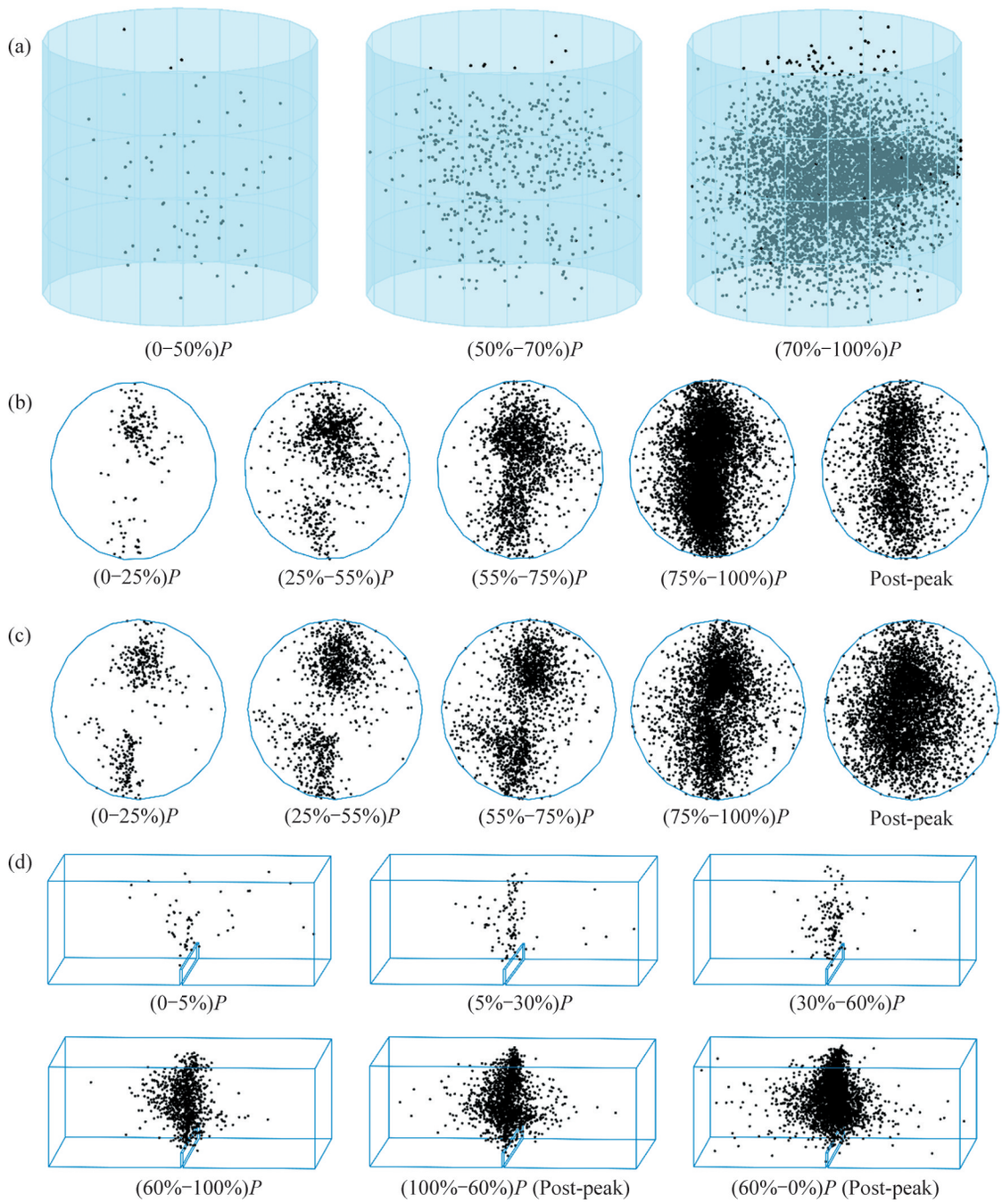

Figure 5 AE spatial distributions at different loading stages in different tensile tests: (a) Direct tensile test (UT-2); (b) Brazilian test with simplified ISRM standard (d-3); (c) Brazilian test with China standard (f-3); (d) Three-point-bending test (b-4)

However, due to the influence of the steel bar, only a small amount of AE counts occurred at the end of the specimen in the early stage of loading caused by compression in the Brazilian test with China standard. So, the number of AE counts is lower than that of Brazilian test with simplified ISRM standard, but higher than that of the direct tensile test and the three-point-bending test. From Figure 5(b), the AE events in the Brazilian test with simplified ISRM standard started to be observed at the center of the disc specimen at the loading stage of (55%−75%)*P*, which indicates the initiation of the tensile fractures at the center of the disc specimen. From about 75% of the peak stress, the microcracks at the center are connected with the microcracks near the contact surfaces, and finally the macroscopic failure of the

specimen along the loading direction is developed. Accordingly, a rapid increase in the cumulative AE counts is noticed (Figure 4(b)). The AE events appearing at this stage have a relatively high energy.

Unlike the Brazilian test with simplified ISRM standard, due to the stress concentration induced by the steel bars between the plat and specimen in the Brazilian test with China standard, the concentration of the AE events around the loading point is more evident (Figure 5(c)). The AE events are observed to expand from the loading point to the center of the disc specimen. The AE events at the center of the specimen are detected clearly not until the stress level is up to 75%*P*. Overall, the distribution of AE events is more linearly centralized along the loading direction during the peak stress loading stage. At the post-peak stage, the AE events are more decentralized and distributed inside the specimen. This suggests that the connecting fracture has been formed during the peak stress loading stage. The AE events after peak stress are mainly induced by the compressive deformation of the disc specimen.

In three-point-bending test (Figure 5(d)), some AE events are detected at the tip of the notch at the beginning of the test (0 − 5%*P*), indicating that the initial fracture occurrs at the notch tip. With increasing compression, the AE events accumulate along the vertical path between the loading point and the notch tip. From about 60% of the peak stress, a large number of AE events with high energy are detected, and a sharp increase in cumulative AE counts is observed (Figure 4(d)). During the peak stress loading stage, the rock specimen is not completely failed, and still has a certain bearing capacity. A large amount of AE events are detected during the post-peak failure process with the increasing deformation. Furthermore, a distinct Kaiser effect could be observed in the three types of tensile tests. Before peak stress, no obvious AE event is detected during the unloading stage or when the loading stress is lower than the maximum stress level of the previous loading − unloading cycle. In the post-peak stage, many AE events are detected only when the axial deformation during loading is larger than the maximum axial deformation of the previous loading −unloading cycle.

When the stress level is close to the peak strength of rock specimens, the macroscopic deformation and failure occur due to the accumulation and propagation of microcracks inside the specimen, and the induced AE events are observed to have high energy. From the experimental results, the energy amplitude of the majority of the AE events at the peak stress loading stage is observed to be higher than 50. Figure 6 shows the spatial distribution of the total AE events, the AE events with energy amplitude > 50 and the failure pattern of the representative specimens in different tensile tests. It can be noticed that the AE events mainly occurred and concentrated along the failure surface during the three types of tensile test, especially for the AE events with high energy (energy amplitude >50). Rock salt is composed of crystalline grains. Under the direct tensile stress, the tensile stress on the specimen is prone to form stress concentration at the contact part of each crystalline grain, where micro-cracks initiate and expand to form a tensile failure (Figure 6(a)). Under the indirect tensile stress (Brazilian test), due to the influence of flat steel (simplified ISRM standard) and steel bars (China standard), the failure must occur along the predetermined failure surface, so that the applied load must split all the crystals on the failure surface. Affected by the two different contact methods of loading, large-area compressive shear failure occurs at the two ends of the rock salt specimen in the Brazilian test with simplified ISRM standard, and the tensile failure occurs only in the middle of the specimen. The opening of tensile failure is much larger than that of the specimen loaded with steel bars, and the failure pattern is relatively curved, close to an S-shaped open failure (Figure 6(b)). In the Brazilian test with China standard, the specimen is loaded with a steel bar, which caused the tensile failure to penetrate through both ends of the specimen. The failure pattern is relatively regular and straight (Figure 6(c)). In the three-point-bending test, the maximum tensile stress occurs at the tip of the notch, where the crack initiates and develops to cause the tensile failure (Figure 6(d)).

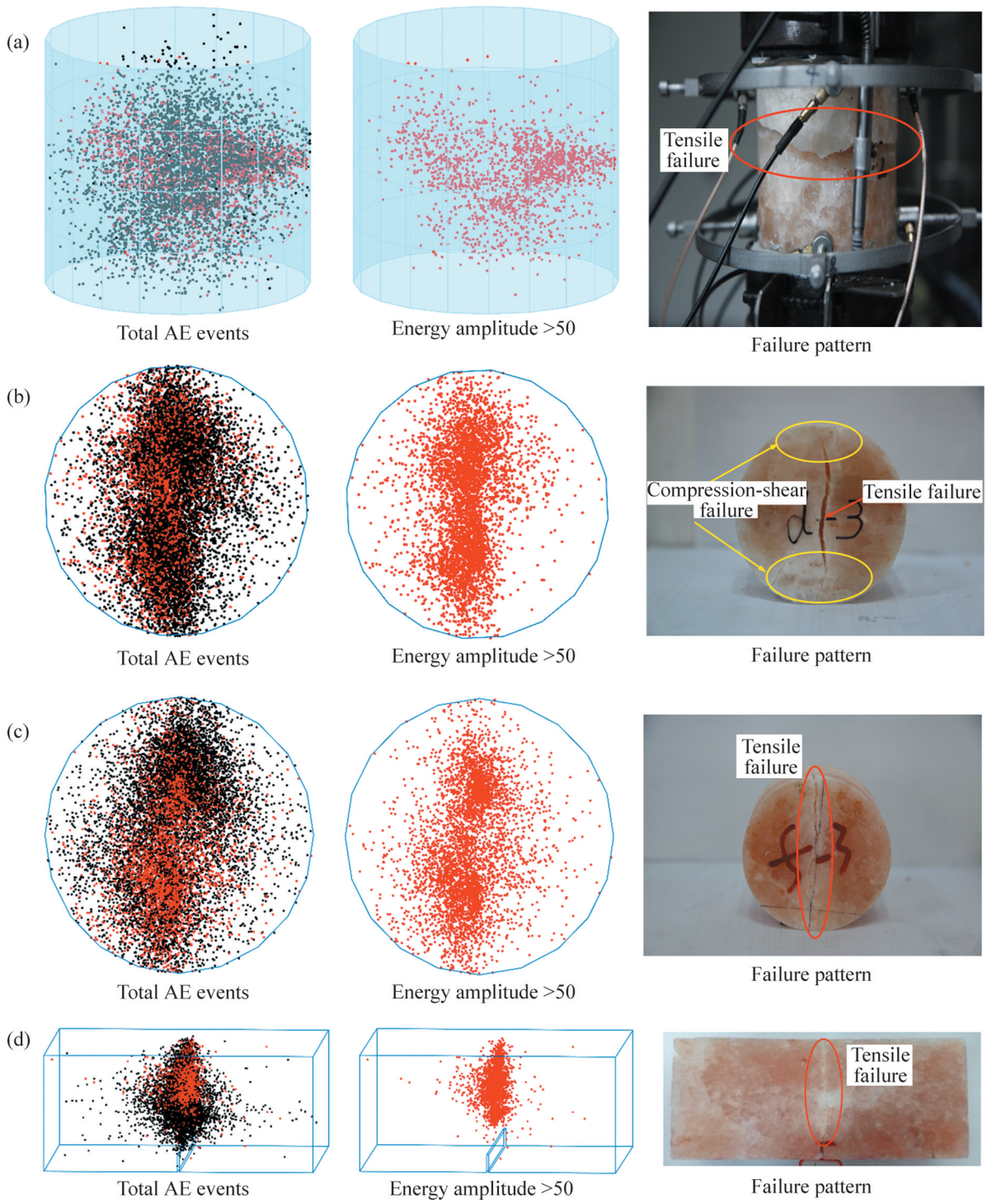

Figure 6 AE spatial distributions and failure patterns for different tensile tests: (a) Direct tensile test (UT-2); (b) Brazilian test with simplified ISRM standard (d-3); (c) Brazilian test with China standard (f-3); (d) Three-point-bending test (b-4)

4 Discussion

The direct tensile test is the most fundamental and straightforward method for determining the tensile strength of rocks. The rock specimen in direct tensile test is under a simple tensile stress condition, and the tensile strength determined by direct tensile test is more reliable and real. The only drawback of direct tensile test might be the high requirements for experimental setup and rock specimens. Therefore, the direct tensile test is preferred if an experimental apparatus is available to provide an axial tension.

Brazilian test, as the indirect tensile test, is the most commonly used tensile test method. But the tensile strength obtained by this method is significantly higher than that obtained by the direct tensile test. In Brazilian test, the contact area between plate and specimen is increased significantly with the increase of loading stress. Therefore, the large contact surface allows an end restraint effect to the rock specimen in Brazilian test, which leads to a relatively high tensile strength. Comparing the results of the two kinds of Brazilian test with different standards, the tensile strength obtained by tests is closely related to the type of loading contact. In Brazilian test with China standard, the two steel bars placed between the plat and specimen provide a symmetric line loading, which may partly eliminate the influence of end restraint effect. Therefore, the indirect tensile strength determined from Brazilian test with China standard is less than that determined from Brazilian test with simplified ISRM standard, meaning that the Brazilian test with China standard in an indirect tensile test method is much closer to the direct tensile test.

According to the experimental results, the tensile strength determined by three-point-bending test is the closest to the tensile strength determined by direct tensile test. Meanwhile, the AE events are first detected at the tip of the notch at the beginning of the three-point-bending test, indicating that the initial fracture occurred at the notch tip. Although the rock specimen is not completely under a tensile stress condition, the notch tip at the center of the bottom surface of specimen where the initial fracture occurs is under a pure tensile state. That is the rock failure in three-point-bending test is caused mainly by tensile stress. Moreover, the three-point-bending test can be easily conducted with a compression test machine, and the specimen can be easily prepared with a simple geometrical shape. We therefore think that the notched three-point-bending test is another alternative to obtain the tensile strength of rocks.

Considering the stress cycle of loading and unloading in underground salt cavern, the rock salt will undergo the tension − compression cycles, and the tensile strength will be affected by the stress path, which has not been discussed in depth in this paper. Based on the analysis and discussion of the test methods of the tensile strength of rock salt in this paper, we also expect to consider the influence of the tension − compression cycles in the further research, so as to provide more reliable support for the underground rock salt project.

5 Conclusions

Focusing on the effect of different tensile test methods on the tensile strength of rock salt, the direct tensile test, Brazilian test with simplified ISRM standard, Brazilian test with China standard, and three-point-bending test were performed. The main results are as follows.

1) The average tensile strengths of rock salt determined from direct tensile test, three-point-bending test, Brazilian test with simplified ISRM standard and Brazilian test with China standard are 0.84, 0.81, 1.97 and 1.15 MPa, respectively. The Brazilian test with ISRM standard measures the highest tensile strength. The indirect tensile strength determined by three-point-bending test is much closer to the tensile strength determined by direct tensile test.

2) The microcracking process during the three types of tensile test can be clearly illustrated by the evolution of cumulative AE counts and AE energy rate and the spatial distribution of AE events. The AE events mainly occur and concentrate along the failure surface, especially for the AE events with high energy amplitude. For Brazilian test, the AE events are mainly localized at the compressive zone near the loading surface at the beginning of the test, which could be attributed to the close of the intrinsic microcracks inside the specimen under compression. For three-point-bending test, the AE events are first detected at the notch tip which is under a pure tensile state.

3) Based on the tensile strength determined by three-point-bending test and the AE evolution characteristics, the three-point-bending test may be a good option to obtain the tensile strength of rock salt except direct tensile test.

Contributors

LIU Jian-feng developed the overarching research goals and edited the draft of manuscript. WANG Chun-ping conducted the literature review and wrote the first draft of manuscript. WANG Lu

revised and wrote the manuscript. RAN Li-na edited the manuscript. DENG Chao-fu conducted the experiments.

Conflict of interest

LIU Jian-feng, WANG Chun-ping, WANG Lu, RAN Li-na and DENG Chao-fu declare that they have no conflict of interest.

References

[1] HOATHER H, CHALLINOR D. The use of salt cavities for the disposal of waste [C]// Proceedings of SMRI Fall Meeting. Hannover, Germany, 1994: 325.

[2] THOMS R, GEHLE R. A brief history of salt cavern use [C]// Proceedings of the 8th World Salt Symposium. The Hague, 2000: 207–214.

[3] GILLHAUS A. Natural gas storage in salt caverns-present status, developments and future trends in Europe [S]. Germany, 2007.

[4] LIANG W, YANG C, ZHAO Y, et al. Experimental investigation of mechanical properties of bedded salt rock [J]. International Journal of Rock Mechanics and Mining Sciences, 2007, 44(3): 400–411. DOI: 10.1016/j. ijrmms. 2006.09.007.

[5] WANG Gui-jun, GUO Kang-mei, CHRISTIANSON M, et al. Deformation characteristics of rock salt with mudstone interbeds surrounding gas and oil storage cavern [J]. International Journal of Rock Mechanics and Mining Sciences, 2011, 48(6): 871–877. DOI: 10.1016/j. ijrmms. 2011.06.012.

[6] MANSOURI H, AJALLOEIAN R. Mechanical behavior of salt rock under uniaxial compression and creep tests [J]. International Journal of Rock Mechanics and Mining Sciences, 2018, 110: 19–27. DOI: 10.1016/j. ijrmms. 2018. 07.006.

[7] ISTVAN J A, EVANS L J, WEBER J H, et al. Rock mechanics for gas storage in bedded salt caverns [J]. International Journal of Rock Mechanics and Mining Sciences, 1997, 34(3–4): 142. DOI: 10.1016/s1365-1609(97) 00108-1.

[8] XIE H P, LIU J F, JU Y, et al. Fractal property of spatial distribution of acoustic emissions during the failure process of bedded rock salt [J]. International Journal of Rock Mechanics and Mining Sciences, 2011, 48(8): 1344–1351. DOI: 10.1016/j.ijrmms.2011.09.014.

[9] SRIAPAI T, WALSRI C, FUENKAJORN K. Effect of temperature on compressive and tensile strengths of salt [J]. Science Asia, 2012, 38(2): 166. DOI: 10.2306/scienceasia 1513-1874.2012.38.166.

[10] WANG T T, YANG C H, MA H L, et al . Safety evaluation of salt cavern gas storage close to an old cavern [J]. International Journal of Rock Mechanics and Mining Sciences, 2016, 83: 95–106.

[11] LIU J, PEI J, MA K, et al. Damage evolution and fractal property of salt rock in tensile failure [C]// Proceedings of 72nd EAGE Conference: Underground Storage of CO_2 and Energy. Barcelona, Spain, 2010: 105–112. DOI: 10.1201/b11 592-21.

[12] WANG Yu-suo, HU Xiao-zhi. Determination of tensile strength and fracture toughness of granite using notched three-point-bend samples [J]. Rock Mechanics and Rock Engineering, 2017, 50(1): 17–28. DOI: 10.1007/s00603-016-1098-6.

[13] DOU Fa-kai, WANG J G, ZHANG Xiang-xiang, et al. Effect of joint parameters on fracturing behavior of shale in notched three-point-bending test based on discrete element model [J]. Engineering Fracture Mechanics, 2019, 205: 40–56. DOI: 10.1016/j.engfracmech.2018.11.017.

[14] LIU J, WANG C, WU Z, et al. A new approach of rock tension–compression cyclic measurement [J]. Géotechnique Letters, 2019, 9(2): 89–93. DOI: 10.1680/jgele.18.00202.

[15] GOODMAN R E. Introduction to rock mechanics [M]. 2nd ed. New York: Wiley, 1989.

[16] VERVOORT A, MIN K B, KONIETZKY H, et al. Failure of transversely isotropic rock under Brazilian test conditions [J]. International Journal of Rock Mechanics and Mining Sciences, 2014, 70: 343–352. DOI: 10.1016/j. ijrmms. 2014. 04.006.

[17] DAN D Q, KONIETZKY H. Numerical simulations and interpretations of Brazilian tensile tests on transversely isotropic rocks [J]. International Journal of Rock Mechanics and Mining Sciences, 2014, 71: 53–63. DOI: 10.1016/j. ijrmms.2014.06.015.

[18] KHOSRAVI A, SIMON R, RIVARD P. The shape effect on the morphology of the fracture surface induced by the Brazilian test [J]. International Journal of Rock Mechanics and Mining Sciences, 2017, 93: 201–209. DOI: 10.1016/j. ijrmms.2017.01.007.

[19] YAMAMOTO Y, SPRINGMAN S M. Three- and four-point bending tests on artificial frozen soil samples at temperatures close to 0°C [J]. Cold Regions Science and Technology, 2017, 134: 20–32. DOI: 10.1016/j.coldregions.2016.11.003.

[20] LIAO Z Y, ZHU J B, TANG C A. Numerical investigation of rock tensile strength determined by direct tension, Brazilian and three-point bending tests [J]. International Journal of Rock Mechanics and Mining Sciences, 2019, 115: 21–32. DOI: 10.1016/j.ijrmms.2019.01.007.

[21] MELLOR M, HAWKES I. Measurement of tensile strength by diametral compression of discs and annuli [J]. Engineering Geology, 1971, 5(3): 173–225. DOI: 10.1016/ 0013-7952(71)90001-9.

[22] HUDSON J A, BROWN E T, RUMMEL F. The controlled failure of rock discs and rings loaded in diametral compression [J]. International Journal of Rock Mechanics and Mining Sciences & Geomechanics Abstracts, 1972, 9(2): 241–248. DOI: 10.1016/0148-9062(72)90025-3.

[23] ISRM. Suggested methods for determining tensile strength of rock materials [J]. International Journal of Rock Mechanics and Mining Sciences & Geomechanics Abstracts, 1978, 15 (3): 99–103. DOI: 10.1016/0148-9062(78)90003-7.

[24] GB/T50266—2013. Standard for test method of engineering rock mass [S]. China, 2013. (in Chinese)

[25] GB/T 50081—2002. Standard for tests method of mechanical properties on ordinary concrete [S]. China, 2003. (in Chinese)

[26] COVIELLO A, LAGIOIA R, NOVA R. On the measurement of the tensile strength of soft rocks [J]. Rock Mechanics and Rock Engineering, 2005, 38(4): 251 − 273. DOI: 10.1007/s00603-005-0054-7.

[27] SUITS L D, SHEAHAN T C, FUENKAJORN K, et al. Laboratory determination of direct tensile strength and deformability of intact rocks [J]. Geotechnical Testing Journal, 2011, 34(1): 103134. DOI: 10.1520/gtj103134.

[28] LIU Jian-feng, XIE He-ping, JU Yang, et al. Device with position-limit spring for alternating tension-compression cyclic test: US9488560 [P]. 2016-11-08.

[29] JU Yang, XIE He-ping. A variable condition of the damage description based on hypothesis of strain equivalence [J]. Chinese Journal of Applied Mechanics, 1998, 15(1): 43 − 49. (in Chinese)

(Edited by FANG Jing-hua)

中文导读

基于不同拉伸试验的盐岩拉伸破坏及声发射特征研究

摘要：盐岩的抗拉强度是盐穴储气工程中的一个重要参数，由于直接拉伸试验对试验装置和岩石试件的要求较高，导致其测试难度较大，需要探索一种试验简单、测试准确的方法来获得抗拉强度。为此，本文针对盐岩开展了直接拉伸试验、简化ISRM标准巴西试验、中国标准巴西试验和三点弯曲试验，分析了基于不同试验获得的盐岩抗拉强度及拉伸破坏过程中的声发射（AE）特性。结果表明拉伸试验方法对盐岩抗拉强度以及声发射计数、能量和空间分布特征具有显著影响。对比基于不同试验方法得到的抗拉强度及盐岩拉伸破坏特征发现，三点弯曲试验测定的间接抗拉强度与直接抗拉试验测定的抗拉强度更为接近，因此三点弯曲试验可作为除直接抗拉试验外测定盐岩抗拉强度的较好选择。

关键词：盐岩；抗拉强度；声发射；破坏特征